



**Universidade do Minho**  
Escola de Engenharia

Eduardo José Tanque de Pádua Cruz

## **Parallel Interactive Ray Tracing and Exploiting Spatial Coherence**

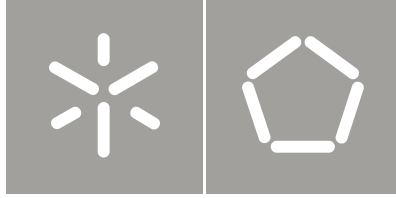
**Parallel Interactive Ray Tracing and  
Exploiting Spatial Coherence**

Eduardo José Tanque  
de Pádua Cruz

UMinho | 2013

Janeiro de 2013





**Universidade do Minho**  
Escola de Engenharia

Eduardo José Tanque de Pádua Cruz

**Parallel Interactive Ray Tracing and  
Exploiting Spatial Coherence**

Dissertação de Mestrado  
Mestrado em Informática

Trabalho realizado sob a orientação do  
**Professor Doutor Luís Paulo Peixoto dos Santos**



# Inscription

---

*"We choose to go to the moon, we choose to go to the moon in this decade and do the other things, not because they are easy, but because they are hard, because that goal will serve to organize and measure the best of our energies and skills, because that challenge is one that we are willing to accept, one we are unwilling to postpone, and one which we intend to win, and the others, too." - John F. Kennedy, 12th of September, 1962*



# Acknowledgments

---

This research project would not have been possible without the support of many people. First and most of all, I would like to express my deepest gratitude to my supervisor, Prof. Dr. Luis Paulo Peixoto dos Santos for accepting me as his student, selecting me for the research grant and for the invaluable offered assistance, support and guidance. My gratitude is also due to the members of the CoLab, who allowed me to participate in a Summer School in the University of Texas – Austin, where I got significant insight on parallel computation, computer graphics and academic research.

I would also like to convey thanks to the Science and Technology Foundation of Portugal (FCT) for providing the financial means to perform this study and to the Department of Informatics of the University of Minho for making available their staff laboratory facilities.

I must also express my gratitude to Dr. Nuno Brito, for his unselfish and unfailing support, pushing me forward to complete this work and help in the review process of this thesis.

I also wish to express my love and gratitude to my beloved family and Filipa, for their understanding and endless love, through the duration of my studies. I will carry you with me wherever I go.

I also thank my Dear Lord, for giving the strengths to continue when matters seemed worthless and always putting the next step of the path so I could reach this goal.





# Abstract

---

Ray tracing is a rendering technique that allows simulating a wide range of light transport phenomena, resulting on highly realistic computer generated imaging. Ray tracing is, however, computationally very demanding, compared to other techniques such as rasterization that achieves shorter rendering times by greatly simplifying the physics of light propagation, at the cost of less realistic images.

The complexity of the ray tracing algorithm makes it unusable for interactive applications on machines without dedicated hardware, such as GPUs. The extreme task independent nature of the algorithm offers great potential for parallel processing, increasing the available computational power by using additional resources. This thesis studies different approaches and enhancements on the decomposition of workload and load balancing in a distributed shared memory cluster in order to achieve interactive frame rates.

This thesis also studies approaches to enhance the ray tracing algorithm, by reducing the computational demand without decreasing the quality of the results. To achieve this goal, optimizations that depend on the rays' processing order were implemented. An alternative to the traditional image plane traversal order, scan line, is studied, using space-filling curves.

Results have shown linear speed-ups of the used ray tracer in a distributed shared memory cluster. They have also shown that spatial coherence can be used to increase the performance of the ray tracing algorithm and that the improvement depends of the traversal order of the image plane.

*Keywords: Ray Tracing, Parallel Computing, Spatial Coherence*

# Resumo

---

O *ray tracing* é uma técnica de síntese de imagens que permite simular um vasto conjunto de fenômenos da luz, resultando em imagens geradas por computador altamente realistas. O *ray tracing* é, no entanto, computacionalmente muito exigente quando comparado com outras técnicas tais como a rasterização, a qual consegue tempos de síntese mais baixos mas com imagens menos realistas.

A complexidade do algoritmo de *ray tracing* torna o seu uso impossível para aplicações interativas em máquinas que não disponham de *hardware* dedicado a esse tipo de processamento, como os *GPUs*. No entanto, a natureza extremamente paralela do algoritmo oferece um grande potencial para o processamento paralelo. Nesta tese são analisadas diferentes abordagens e otimizações da decomposição das tarefas e balanceamento da carga num cluster de memória distribuída, por forma a alcançar frame rates interativas.

Esta tese também estuda abordagens que melhoram o algoritmo de *ray tracing*, ao reduzir o esforço computacional sem perder qualidade nos resultados. Para esse efeito, foram implementadas otimizações que dependem da ordem pela qual os raios são processados. Foi estudada, nomeadamente, uma travessia do plano da imagem alternativa à tradicional, *scan line*, usando curvas de preenchimento espacial.

Os resultados obtidos mostraram aumento de desempenho linear do *ray tracer* utilizado num *cluster* de memória distribuída. Demonstraram também que a coerência espacial pode ser usada para melhorar o desempenho do algoritmo de *ray tracing* e que estas melhorias dependem do algoritmo de travessia utilizado.

Palavras-Chave: *Ray Tracing, Computação Paralela, Coerência Espacial*

<b>Inscription .....</b>	<b>i</b>
<b>Acknowledgments.....</b>	<b>iii</b>
<b>Abstract .....</b>	<b>v</b>
<b>Resumo .....</b>	<b>vi</b>
<b>Index.....</b>	<b>vii</b>
<b>List of Acronyms .....</b>	<b>ix</b>
<b>Index of Figures .....</b>	<b>xi</b>
<b>Index of tables .....</b>	<b>xiii</b>
<b>1 Introduction .....</b>	<b>1</b>
1.1 Motivation.....	1
1.2 Organization .....	2
<b>2 Objectives and Goals.....</b>	<b>3</b>
<b>3 State of the Art .....</b>	<b>4</b>
3.1 Ray Tracing .....	4
3.2 Acceleration Data Structures .....	5
3.3 Rasterization vs. Ray tracing.....	5
3.4 Coherence .....	6
3.5 Processing Packets instead of Single Rays .....	7
3.6 Parallel Ray Tracing .....	9
3.7 Parallel Progressive Ray Tracing.....	11
3.8 Parallel task assignment strategies in the Demand Driven context.....	12
3.9 Ray coherence techniques .....	14
3.10 Space filling curves.....	15
3.11 The Hilbert curve.....	16
<b>4 METODOLOGY .....</b>	<b>19</b>
4.1 iRT Overview .....	19
4.2 Workload decomposition .....	20
4.3 Measuring efficiency of parallelization .....	21
4.4 Static Distribution.....	22
4.5 Static-Cyclic Distribution.....	23
4.6 Dynamic load balance.....	24

4.7	Tasks refinement .....	26
4.8	Non-blocking communication.....	26
4.9	Comparing Scan Line and Hilbert line traversal.....	26
5	RESULTS .....	31
5.1	Experimental Setup .....	31
5.2	Load Balancing .....	31
5.3	Spatial Coherence.....	36
6	CONCLUSIONS.....	43
6.1	Achieved goals.....	43
6.2	Future work .....	43
7	BIBLIOGRAFY .....	45

# List of Acronyms

---

<b>AABB</b>	Axis Aligned Bounding Boxes (Volumes Delimitadores Alinhados pelos Eixos)
<b>ADS</b>	Acceleration Data Structures (Estruturas de Dados de Aceleração)
<b>BVH</b>	Bounding Volume Hierarchy (Hierarquia de Volumes Delimitadores)
<b>DSM</b>	Distributed Shared Memory (Memória Partilhada Distribuída)
<b>IGIDE</b>	Interactive Global Illumination within Dynamic Environments (Iluminação Global Interactiva em Ambientes Dinâmicos)
<b>iRT</b>	Interactive Ray Tracer (Ray-Tracer Interactivo)
<b>Kd-tree</b>	K-dimensional Tree (Árvore K-dimensional)
<b>SM</b>	Shared Memory (Memória Partilhada)
<b>SISD</b>	Single Instruction Single Data (Instrução Única para Dados Únicos)
<b>SIMD</b>	Single Instruction Multiple Data (Instrução Única para Dados Múltiplos)



# Index of Figures

---

Figure 1 - Light Path in Ray Tracing.....	7
Figure 2 - SISD vs. SIMD.....	8
Figure 3 - Scan Line.....	16
Figure 4 - Peano Curve.....	16
Figure 5 - Hilbert Curve.....	16
Figure 6 - First 6 iterations of the 2D Hilbert Curve.....	17
Figure 7 - First four iterations of the 2D Hilbert curve in arc view.....	18
Figure 8 - iRT Pipeline.....	19
Figure 9 - Architecture of iRT.....	20
Figure 10 - Static Distribution.....	22
Figure 11 - Static-Cyclic Distribution.....	23
Figure 12 - Load Distribution with a Static-Cyclic approach.....	24
Figure 13 - Dynamic Load Balancing.....	25
Figure 14 - Task Refinement.....	26
Figure 15 - Bunny - Scan Line.....	27
Figure 16 - Bunny - Hilbert Curve.....	27
Figure 17 - Office - Scan Line.....	27
Figure 18 - Office - Hilbert Curve.....	27
Figure 19 - Sibenik - Scan Line.....	27
Figure 20 - Sibenik - Hilbert Curve.....	27
Figure 21 - Sponza - Scan Line.....	28
Figure 22 - Sponza - Hilbert Curve.....	28
Figure 23 - Bunny - Scan Line.....	36
Figure 24 - Bunny - Hilbert Curve.....	36
Figure 25 - Office - Scan Line.....	36
Figure 26 - Office - Hilbert Curve.....	36
Figure 27 - Sibenik - Scan Line.....	37
Figure 28 - Sibenik - Hilbert Curve.....	37
Figure 29 - Sponza - Scan Line.....	37
Figure 30 - Sponza - Hilbert Curve.....	37





# Index of tables

---

*Table 1 - Coherence in Primary Rays..... 28*

*Table 2 - Load Balancing – Bunnies..... 32*

*Table 3 - Load Balancing – Office..... 33*

*Table 4 - Load Balancing - Sibenik..... 34*

*Table 5 - Load Balancing – Sponza..... 35*

*Table 6 - Spatial Coherence with Scan Line Traversal..... 38*

*Table 7 - Spatial Coherence with Hilbert Curve Traversal..... 39*

*Table 8 – Gain of Traversing the Image Plane with the Hilbert Curve against Scan Line..... 39*

*Table 9 - Exploiting Coherence with Scan Line Traversal..... 40*

*Table 10 - Exploiting Coherence with Scan Line Traversal..... 41*

# 1 Introduction

---

## 1.1 Motivation

Ray tracing based renderers simulate global illumination and physically based light transport effects, simulating the path that real light photons make. This rendering outputs high fidelity images used in a predictive manner [1]. Being able to represent realistic light effects is important in many applications such as the movie industry, light architecture and generation of complex virtual environments. These applications often have interactivity requirements, which implies very fast response times when calculating the light effects. Given the fact that the ray tracing algorithm is computationally demanding, such is not possible in current computers without using special purpose hardware.

Other techniques, such as rasterization approaches are significantly faster because they aggressively exploit spatial coherence and perform simplifications and assumptions at the cost of less accurate and realistic lightning effects. Traditionally in ray tracing, as observed by Whitted [2], each ray can be traced independently from the others and thus less assumptions are made, which increases its versatility but also increases the computational demand. In this thesis, a study is made about coherence properties available in ray tracing and explores techniques that take advantage of these properties, to reduce the required computational effort and increase the overall performance. In particular, the use of space filling curves as an alternative to the traditional image plane traversal order is proposed.

More efficient algorithms can increase the obtained frame rate but the result is bond to the processing limits of the hardware. This limitation can be overcome by the use of parallel computation, using multiple machines to increase the computational power. Given the extreme parallel nature of the ray tracing algorithm, it is expected that the performance of the algorithm can scale linearly with the increase of the computational power.

Parallel computation entails issues such as communication latencies, load imbalance and suboptimal work decomposition. Resorting to techniques such as non-blocking communication, dynamic workload distribution and preemptive work decomposition can mitigate these issues.

## **1.2 Organization**

In chapter 2 an introduction to the theme of this thesis is given and its goals are set. On chapter 3 a revision of the state of the art is made, identifying and analysing approaches already at use. This analysis brings support to the decisions and approach taken during this research as described in chapter 4. Also in this chapter will be described the methodology and implementation used. In chapter 5 the results from the research experiments will be presented and analysed. The work from these chapters leads to the conclusions proposed in 6

# 2 Objectives and Goals

---

Interactive frame rates can only be achieved by increasing the computational power and/or resorting to optimization techniques that improve the performance of the ray tracing algorithm. In this thesis we propose to look into both. In the early days of ray tracing the use of DSM clusters was appealing because the nature of the algorithm required more computational power than the one existing in single workstations [3], [4]. With the steady increase of computational power, the power of clusters came into single workstations and research started to focus on SM architectures. However, these approaches require low-level design and are prone to errors. By exploiting approaches with message passing interfaces, traditionally used for clusters, they remain valid for any environment that supports such interfaces. Currently they can be executed seamlessly in single or multiple workstations, making such approaches highly scalable and flexible.

This thesis proposes to study whether the image space traversal order can influence the success of techniques that exploit ray coherence. Traditionally, the image plane is traversed in scan line order, but this approach is bound to one dimension and inherently loses coherence in a bi-dimensional space. Space filling curves have been studied before [5] as means of covering multi-dimensional discrete spaces with a single line, and the great spatial coherence exhibited by some of these curves has been applied to several fields, such as mathematics, image processing and compression, cryptology, algorithms, scientific computing, parallel computing, geographic information systems and database systems [6]. For that matter, special purpose optimizations will be studied and implemented in order to evaluate if the traversal order of the image plane can be used to exploit spatial coherence existing in ray tracing.

# 3 State of the Art

---

## 3.1 Ray Tracing

Ray tracing one frame containing only static scenery with a pre-computed acceleration structure is an embarrassingly parallel task [1], [7]. Tracing rays is a recursive process that has to be carried out for each individual pixel separately. One of the most expensive parts of the rendering algorithm is the visibility calculation. At least one ray is shot per pixel and in a naive approach each ray would be intersected with all the objects in the scene to determine which is the closest triangle intersecting a given ray. To evaluate the light intensity that an object scatters towards the eye, the intensity of the light reaching that object has to be evaluated as well. Ray tracing achieves this by shooting additional, secondary rays, because when a ray hits a reflecting or transparent surface, one or more new rays are cast from that point, simulating the reflection and refraction effects. A typical image of 1024 x 1024 pixels tends to cost at least a million primary rays and a multiple of that as shadow, reflection and transparency rays.

Ray tracing is thus considered as a computationally demanding algorithm that does not benefit from optimized hardware for its processing. In the past, ray tracing algorithms could only provide interactive frame rates at the cost of limited resolution [8] and simulated shading effects [9].

The present state of available technology provides affordable machines with multiple CPU cores that can work in parallel. The current challenge is to support interactive ray tracing in higher frame rates at higher resolutions, taking advantage of algorithm processing in parallel machines equipped with many cores.

This approach allows support for:

- High complexity scenes that do not fit on the memory of a single machine, such as representations of complex buildings and structures;
- Animated scenes where objects are deformable and move in respect to each other such as hair and clothes of multiple characters;
- Compelling light effects that are not feasible with rasterization approaches such as realistic water and fire effects.

## 3.2 Acceleration Data Structures

The most expensive task in Ray Tracing is identifying which triangles each ray intersects. With the increase of the number of triangles in a scene, the complexity of the algorithm grows linearly,  $O(N)$ . In order to alleviate the computational effort, objects can be organized in ADS. In computer graphics axis-aligned bounding boxes (AABB) are used efficiently to purge objects that will not intersect with the view frustum. Such structures can reduce the ray-triangle intersection tests down to  $O(\sqrt[3]{N})$  [10]. Reshtov applied this same AABB principle to KD-trees [9], achieving interactive frame rates in complex static scenes with millions of triangles. For static scenes, the build time of ADS can be ignored as it will be done once and then reused for the whole duration of the execution, but with dynamic scenes the build and update times must also be considered.

BVH have achieved interactivity in dynamic scenes where objects move and deform by: using a variant of the surface area heuristics SAH algorithm - traditionally used in KD-trees - maintaining the topology of the BVH - just re-fitting the bounding volumes from frame to frame - and tracing the rays in packets, combining the advantages of packet traversal and frustum traversal [11].

## 3.3 Rasterization vs. Ray tracing

One of the main differences between the broadly used rasterization based techniques and pixel-by-pixel approaches such as ray tracing, is the aggressive exploitation of coherence present in primary rays<sup>1</sup>. Approaches based on rasterization are object oriented and empty

---

<sup>1</sup> Light rays calculated from the viewer's perspective, also known as view rays.

spaces are not taken into consideration. Rasterization provides earlier termination conditions, simplifications, assumptions and interpolations that reduce the effort to compute the contribution of each object to the final image at the cost of less accurate images.

The pixel-by-pixel approach provides realistic images because fewer assumptions are adopted. Algorithmic improvements such as specular phenomena, direct illumination and indirect diffuse inter reflections [12], [13] allow to render the desired effects. This approach is more versatile when compared to rasterization [12] but reuses little to none of the information computed previously, implying repeated computation effort that could be avoided if coherence was exploited.

### 3.4 Coherence

Without losing versatility and realism, some optimizations can be applied in ray tracing by exploiting the spatial coherence existent among neighbouring rays. Although light emitted from the light source and travels through reflections and refractions to the viewer's eyes<sup>2</sup>, rays that do not reach the viewer's eyes are not considered relevant when generating a frame. In order to avoid processing rays that will be discarded, the light rays are generated from the viewer plane and travel until the various light sources.

In typical ray tracers, the rays are not traced randomly. There exists a substantial coherence in rays that are traced, i.e. there are common characteristics to most or all of the rays. This coherence is particularly strong for primary rays but it is also present for hard shadow rays<sup>3</sup>, soft shadow rays and other kinds of secondary rays [12]. In orthogonal projection, the primary rays have the same direction and the origins varying slightly in their neighbourhood. In a perspective projection, primary rays share the same origin and the direction varies smoothly in their neighbourhood. This is demonstrated in Figure 1, depicting how the rays that originate from the same image region often represent the same objects or objects that are close in the 3D space of the scene. This assumption is also true for shadow regions that are often created by the same object or objects that are close together.

---

<sup>2</sup> In 1604, the German astronomer Johannes Kepler published "*Astronomia pars Optica*", enunciating as principle that light rays travel from an object to the eye and not the other way around.

<sup>3</sup> A shadow can be divided in two main parts: the umbra and the penumbra (there is also antumbra but usually it has no relevance in computer graphics). Umbra, known as hard shadow, can be described as the darkest part of the shadow, corresponding to areas fully occluded from a given light source and represented as black. Penumbra, known as soft shadow, is partially occluded regarding a given light and is represented by variable scales of darkness. Although hard shadows seldom produce a realistic shadow, they are considerably cheaper to generate than soft shadows. At the time of writing for this thesis, soft shadows were not implemented and we consider "shadows" as hard shadows.

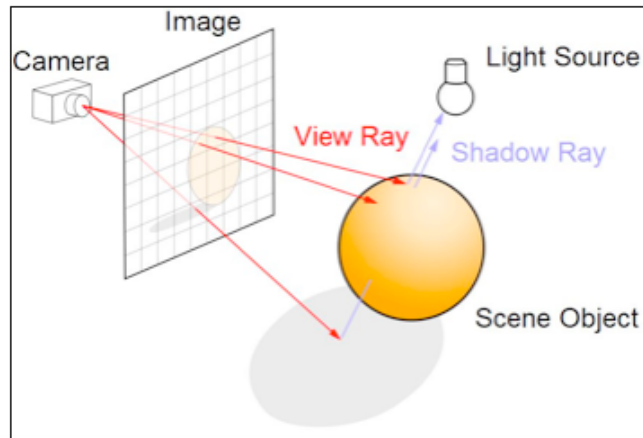


**Figure 1 - Light Path in Ray Tracing**

Ray-tracers traditionally traversed the image plan in a scan line order. The scan line traversal sequence breaks the ray coherence at the end of each line. As this approach only explores one dimension then it might not be the most efficient method. As shadow rays are generated from primary rays, the order by which primary rays are generated directly affects the order by which shadow rays are processed. Spatial coherence and the impact of the traversal algorithm are further explained in section 3.9.

Just for low to median frequency reflection rays, because rays are shot “randomly” in a hemisphere, coherence is not obvious and thus not trivial to explore. Common techniques used to exploit rays coherence are based on aggregation techniques that group rays in a packet or beam based on the principle that coherent rays will traverse similar paths of the ADS and thrive to test them individually as late as possible, thus reducing the ADS traversal cost.

### **3.5 Processing Packets instead of Single Rays**

Modern high performance ray tracers employ the spatial coherence approach to reduce computational costs. Current systems can employ ray aggregation techniques, combining several rays into a packet and/or frustum<sup>4</sup>. The first enunciation of this technique was given by Wald et al, proposing to trace rays in bundles of four through a KD-tree and use of SIMD instructions to process these rays in parallel [14].

Ray aggregation techniques provide advantages for operations such as memory accesses, function calls and traversal computations. This technique permits the use of SIMD instructions

---

<sup>4</sup> Frustum is the portion of a solid that lies between two parallel planes cutting it. In the context of this thesis it refers to the three dimensional region that is visible on the screen.



to gain greater performance from the CPU. Tracing rays with SIMD still requires performing the traversal steps with SISD.

Nunes implemented a SIMD approach in iRT [13], using a packet of four rays, i.e. a set of four floating point values and a four times speedup was expected as depicted on Figure 2. However, the vectorial version is only capable of achieving speeds of 2.8 to 3.7 times faster than the scalar version. Compared to the traditional scalar method, there exist no disadvantages or limitations on this optimization other than the reordering of computation tasks.

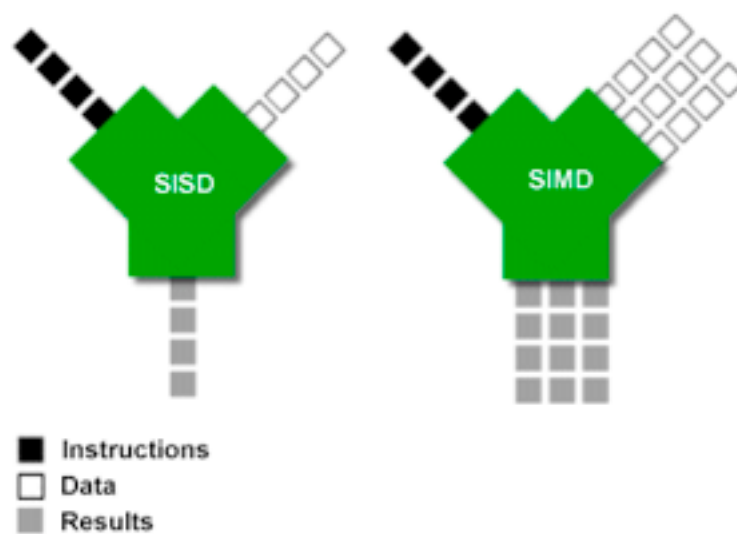


**Figure 2 - SISD vs. SIMD**

Dmitriev et al [15] proposed a broader concept of ray packing using frustum and interval arithmetic-based techniques to avoid traversal steps or primitive intersections based on conservative bounds of the packet of rays. Using the boundaries of the packets of rays, the intersection of all the rays in the packet could be avoided if the full packet misses the triangle.

Reshtov has recently shown that even better performance could be achieved by building a customized frustum at each leaf cell to exclude currently inactive rays [16]. He applied this concept to a KD-tree traversal and used an arithmetic process based on “inverse frustum culling” to cull complete sub trees during the traversal. This concept was later extended to grids and BVH’s, as all of these contexts are sub-cases of AABB [17]. Although additional research is required for improving the less coherent rays, packets and frustum techniques are currently the method of choice for obtaining real-time performance.

### 3.6 Parallel Ray Tracing

Ray tracing supports independence of ray paths, thus being possible to parallelize the computation of its paths. Interactive ray tracing is often achieved by resort to multilevel parallelism such as sampling strategies, exploitation of memory locations and rays coherence [12], [18].

In 2006, Parker et al. stated that “Almost ten years after the first interactive ray tracer was introduced on a massive super computer, the necessary compute power to solve the same visualization problems will be available on a workstation sized system.” [7]. This fact was based on the improvement of individual processing power in modern CPUs. Besides this processing capability increase, Manta has also exploited the emergent tendency of workstations with multiple cores, providing a modular highly scalable parallel pipeline and adopting SIMD instructions for vectorial processors. This modular pipeline gives the entire system additional flexibility as new modules can be easily added or altered without the need of code refactoring. As depicted below in Figure 3, Manta’s pipeline describes the stages necessary to render a single frame.

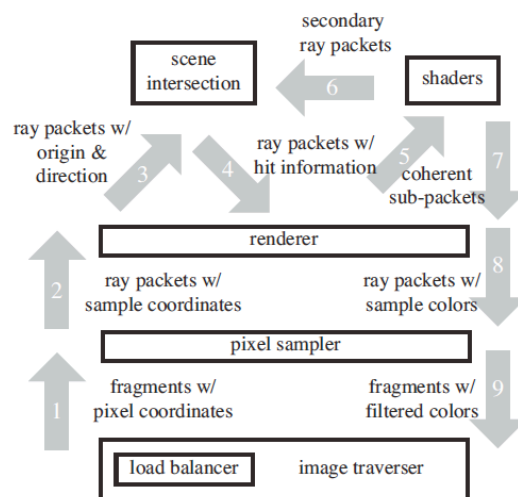


**Figure [7] - Manta's Pipeline for asynchronous rendering**

Exception made for the load balancer, this figure represents a normal single threaded ray tracing pipeline. Although the load balancer is represented as single block, it should be perceived as three separate steps. First, the inherently load balanced tasks such as the pixel sampling or packets construction are scheduled, followed by the load imbalanced tasks such as rendering a packet or image deployment (usually only done by a single thread). After these

two steps, all threads dynamically balance the remaining workload. This way all threads get similar amounts of work and the idle time at the threads-barrier is substantially reduced. With the adoption of this pipeline, the threads synchronization happens only once per frame at the end of each rendering loop. However, this method introduces a one-frame latency between the image being rendered and outputted. If the frame rate is higher than ten frames per second, this latency will hardly be perceived. Actually the one-frame latency allows that synchronization happens at a single barrier, substantially simplifying interactions with the scene. Interactions such as camera movements or scene animations require image displacement and ADS restructuring, if these changes would be taken into consideration within a frame generation then the work effort could be loss due to call-backs or images that become incoherent.

Another important and interesting aspect of Manta's implementation is the adopted data structure known as wide ray packets. Besides being used to communicate between the different modules, each packet contains basic ray information as well as certain properties common to all rays in the packet, such common origin or normalized direction vector. Besides maintaining some degree of coherence among the rays that allow special optimizations, this structure is designed for vectorial calculation. SIMD instructions usually require a vertical data layout. To avoid costly memory re-arrangement, these packets accommodate the data fields vertically so they can be directly loaded in the SIMD registers and uses horizontal access methods so a horizontal layout can also be assumed at the cost of a slight performance penalty.

The size of these packets is not bounded to a specific machine's SIMD width or load balancer tile size. In the case of Manta, the size can vary up to a maximum of 64 rays, which was found to achieve the best performance because the entire packet can fit in the L1 cache [7]. With a variable packet size and careful design of the packet's data layout, splitting into smaller packets can be made so that coherence of each packet is kept.

The load balancer along with thread-bounded ray packets and the pipeline referred above by Manta allows deploying as many threads as desired without the need of reprogramming, scaling almost linearly up to 64 processing units (92%) and achieves 82% efficiency with 126 processors.<sup>5</sup>

---

<sup>5</sup> Results obtained for the model "Boeing 777" with 350 million triangles in an Itanium2 SGI super computer.

### 3.7 Parallel Progressive Ray Tracing

Given the extremely demanding nature of the Ray Tracing algorithm, sampling techniques can be used to alleviate the overall workload, interpolating some of the values instead of pure ray tracing. Usually there are regions of a given frame where the resulting output barely varies, such as in backgrounds or large uniform surfaces, and for these regions, one requires only to compute some of the pixels to estimate the overall characteristics for the surrounding pixels. In fact, this technique is widely used in rasterization-based approaches at the cost of slightly less accurate images.

The quality of the generated images through sampling approaches directly depends on the sample generator algorithm and associated sampling frequency. A usual approach is based on grids. If the grids are too wide then some features such as a light switch on a wall could be discarded and produce aliasing, while too fine grids would render images with better quality but the overhead introduced could eventually produce worst performance than an approach without sampling. A usual solution for this problem is the use of non-uniform adaptive sampling, generating a sample pattern tailored to the image content [19], [20]. This approach uses regular coarse pattern on most pixels, but on regions with high variance, such as edges and silhouettes, a high-density pattern is used. This refinement is done progressively and detail is added to the image gradually, trading aliasing for some noise, which is often negligible.

In a general manner, generators should ensure that larger regions are refined before smaller ones, in order to locate isolated features, and regions with higher intensity variance should be sampled first, to assure anti-aliasing. Refinement should occur until a particular level of the image quality is reached, for instance a defined number of samples, or until a given time limit is passed to allow achieving a desired frame rate. Alternatively to stochastic subdivision, other sample approaches can be used, such as division of image plane division through 2D split planes [21] or Delaunay triangulations [22], [23].

Eldar et al. [23] brought a new method named Farthest Point Strategy for progressive image acquisition, which approximates the whole image at each sampling stage. Notkin et al. [24] extended this approach to parallel ray tracing, parallelizing the inherently sequential algorithm of progressive sampling while thriving to achieve similar image quality with the same number of samples as the sequential version.

Notkin et al. used a generator based on Elder's Delaunay generator and defined tasks as a pair of parameters: the image region, where tiles have a fixed size, and a number of samples, that are variable. As a pre-processing stage, tasks are assigned in a round robin manner and a local image complexity and variance is estimated in parallel by each processor. By multiplying the estimated variance with the time the CPU took to complete the pre-processing stage, a weight metric has been defined. Such weights are sent to the master node that strives to provide a uniform weight distribution that reassigns the tiles by the available processors. This tile distribution will remain unchanged until the end of the frame.

After the pre-processing stage, new tasks are to be assigned dynamically using a Demand Driven approach, gradually decreasing the task size to prevent big workloads in the last samples of each frame<sup>6</sup>. Based on the principles mentioned above for a good sample generator (large and/or big intensity variation regions should be refined first) the master thread assesses a weight for every tile and assigns the slave threads to process the heavier tiles first. Once the goal number of samples has been achieved then the results are collected by the master node, which reconstructs the image.

For a 26-processor count, a speed up of 23.8 was achieved and registered a 15% of load imbalance. Although not achieving a linear speed up, the quality achieved was extremely high and had less than 5% of image resolution loss, which is barely perceivable. For this approach to be tested the scenes were assumed to fit a single's machine memory and this scenario is not always true on parallel ray tracing systems.

### **3.8 Parallel task assignment strategies in the Demand Driven context**

When dividing and balancing a given work load, the size of each task becomes an important factor on the resulting performance. A sub-optimal task size splitting will bring an inefficient overhead and thus cause a loss of performance. When choosing the task sizes, the extreme situation occurs when tasks are the smallest possible, i.e. at the level of one pixel size, which allows perfect load balancing. However the number of requests is significantly higher than the

---

<sup>6</sup> The problem of big tasks being assigned at the end of each frame is referred with greater detail in section 4.7

workers and then leads to overheads such as latency<sup>7</sup>. On the other extreme there exist as many tasks as workers, which results in minimal overhead but more prone to load imbalances. In [25], Plachetka analyses how the task size can be determined based on the image space sub-division and the number of available processors. Then, he proposes an anti-aliasing approach with solutions for scenes that do not fit the available memory of each processor.

Plachetka has experimentally shown that subdividing the tasks in chunks of the size of one column in scenes where the maximum ratio ranges between the computation times of two image regions of the same size is between 2.5 and 4 will yield the best results. Traditionally only one primary ray is spawned per pixel. This might lead to aliasing effects, and anti-aliasing requires spawning more rays per pixel when the difference between a given pixel and its neighbours exceeds a given threshold. Given that the image space is subdivided, the border regions present some challenges: either re-sampling is done on both regions, leading to duplicate work, or communication must exist between the processes holding the different image regions. Plachetka postulated that non-critical regions should be processed first and then process the critical regions afterwards as independent tasks. This approach reduces the duplicate computation and communication effort between the two processes. As anti-aliasing tasks become interleaved with standard tasks, no overhead is added to the process and improves load balancing when the ratio between the computational efforts of different regions is underestimated.

Dividing tasks based on the image region is suitable when the whole scene fits a single processors memory. But when the scene is too complex then it must be divided among the existing nodes. When dividing the tasks, the master node parses the scene, identifying meshes that would not fit the processor memory. Each mesh is then assigned to the processor currently with the lowest memory load and that processor will become the owner of it. The owner node will keep the mesh in memory. The remaining nodes will process the mesh and update their bounding volume hierarchy and keep the information regarding the ownership and then release the mesh's data. Should a processor require a mesh that is not in memory, it requests the mesh from the owner, which has the mesh data already pre-packed. Should the processor not have enough memory to load the requested mesh, the least recently used object will be released, so space is made for the mesh. The mesh can be later released, if memory is

---

<sup>7</sup> Latency is the overhead of assigning one task, i.e. the required time to transmit a message, plus the time of packing and unpacking it. Although it is usually considered constant, often that is not the case, for instance, if simultaneous messages arrive at the same time.

needed for other structures, but data that might later be required for other processes, such as shading, is saved.

With his experiments he postulates that the referred approaches are scalable and bring higher speed-ups. When comparing the approach without anti-aliasing against the anti-aliased approach then performance begins only to decrease after 40 processors are active. As for the objects in memory, the experiments shown that if at least 20% of the scene can be kept in memory, then the algorithm keeps performing above average on a scalable manner. If the available memory size reduces, requests for object data dramatically increases, significantly decreasing the performance and scalability of the algorithm.

### **3.9 Ray coherence techniques**

It has been previously described in section 3.5 that rays can be grouped in packets in order to reduce the costs of traversing the ADS. The quality of these packets strongly depends on how the rays are grouped. In order to better understand the existing level of coherence, individual rays are studied rather than packets.

The coherence existing between the rays directly depends on the order under which they are generated, which is traditionally done in a scan line traverse of the image plane. This approach limits the exploration of coherence to a single dimension and inherently breaks the coherence at the end of each line.

Considering that reloading an object or part of the ADS to higher levels of the memory hierarchy has an associated cost, an ideal traversal sequence of the image plane would be one that visits all the pixels in the entire area of each object before moving on to the next one, allowing to explore coherence in two dimensions.

Knowledge of the projection area and position of an object beforehand can become too costly and unfeasible to implement, especially if applied to the context of a real-time application.

For the purpose of this thesis, we define two assumptions:

- Information of the projection area and position are unavailable
- Traversal sequence is fixed rather than adaptive

Having these assumptions in consideration, it was defined that selection should be based solely upon the shape of the image plane traversal line.

### 3.10 Space filling curves

Unlike data sets of a single dimension where the algorithms for sorting and traversing are usually trivial and straightforward, multidimensional data sets require more complex operations. For this reason alone, single dimension processing could be preferred over multiple processing dimensions. However, while values can be closely grouped at one of the dimensions, they could still be far apart in other dimensions. Furthermore, it is not a trivial task to choose which dimensions should be preferred.

The space-filling curves algorithm is used for ordering and traversing multidimensional data. It was formulated by Peano in 1890 and consists of continuous self-similar functions that map a single dimension interval to a multiple dimensional set. By convention, space-filling curves are defined as contiguous mappings from the unit interval to n-dimensional hypercube units. It can also be defined as a curve that passes through every point in an n-dimensional space once and once only in some particular order according to some algorithm.

As such, they express graphically a mapping between one-dimensional values and the coordinates of a point, regarded as a multidimensional value. Points are placed in a sequence according to the order under which the curve passes through them. Although the concept of fractal modelling was unknown at the time, Peano curves are fractals and thus considered self-similar at multiple levels or resolutions. This implies that if any advantage is achieved with these curves at a given scale, they will maintain the same advantage at any given scale.

Such curves tend to be good for preserving locality: points close together with respect to the Euclidean distance in the multidimensional matrix tend to be close together in the linear ordering defined by the curve. Out of the 272 possible Peano curve definitions [26], the Hilbert curve appears as the one of greater advantage for image plane traversal. These advantages were demonstrated through solid locality in [6].

Hilbert curves found application in a variety of fields that includes:

- Mathematics
- Image processing and compression
- Cryptology algorithms
- Scientific computing
- Parallel computing



- Geographic information systems
- Database systems (to map multidimensional data to linearly ordered external memory and to promote query efficiency)
- Distributed information systems (to partition multidimensional data in such way that data sets that are close in Euclidean space are likely to be allocated to the same or neighbouring processors).

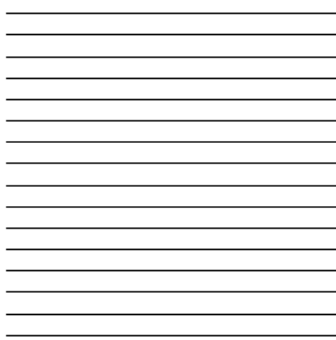


Figure 3 - Scan Line

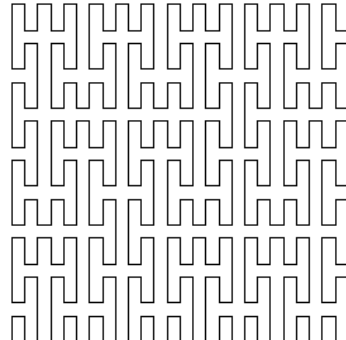


Figure 4 - Peano Curve

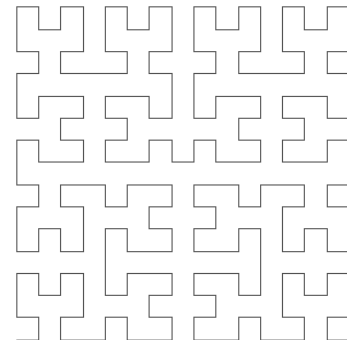


Figure 5 - Hilbert Curve

Douglas Voorhies researched the 2D space filling curves applied on the context of image plane traversal, providing a comparison between the traditional unidirectional scan line, the Peano curve and the Hilbert curve traversal, represented above [27]. He defined a metric of coherence that counts the number of times that a traversal sequence would go inside and outside of an object projection space before all points of a given object have been visited. Assuming that an object's projection in the screen space is a circle, he guarantees that no traversal direction has advantage over any other. He demonstrated that both Peano and Hilbert curves surpassed the coherence measure of conventional scan line traversal. Results have shown that the Hilbert curve provides better coherence results than the Peano curve. Given the fractal property previously referred, it is expected that for any given image, the traversal of the image plane with the Hilbert line should outperform the traditional scan line traversal order in terms of coherence.

### 3.11 The Hilbert curve

Below are represented the first six iterations of the 2D Hilbert curve. One can observe the self-similar nature of such curves where each level of the curve is composed of multiple, smaller

copies of previous levels that are oriented in various patterns. Components of a curve expand in a predictable way to multiple components of the next level.

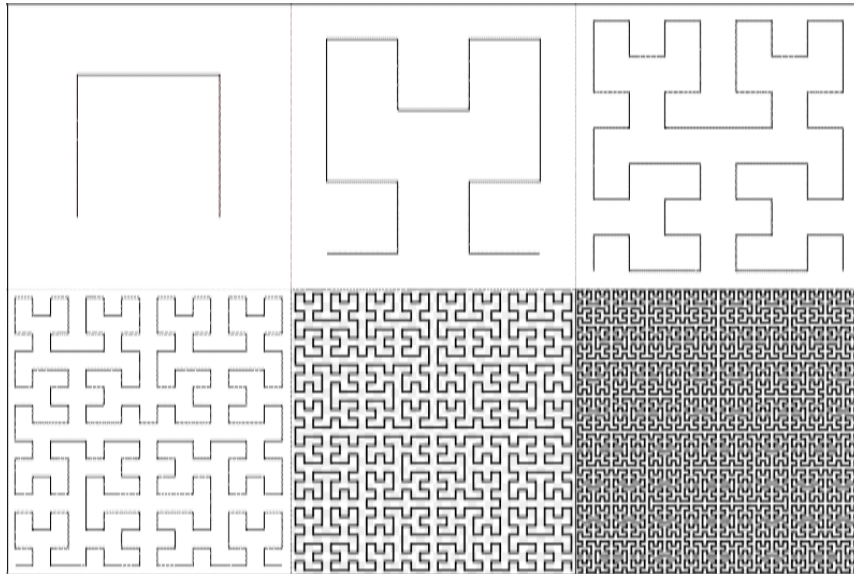


**Figure 6 - First 6 iterations of the 2D Hilbert Curve**

In formal terms, consider an N dimensional lattice with  $2^m$  points per dimension such as:  $P = B^m * \dots * B^m$ , where  $B^m = \{0,1\}$

A standard Hilbert index is a function  $H : P \rightarrow B^{n*m}$ , which maps each point to each index on the Hilbert Curve when it passes through the lattice. The traditional recursive geometric construction of the two-dimensional Hilbert Curve can be defined in four steps. We consider the shape  $\square$  as the base curve that passes by four cells:

- Place a copy of the curve rotated  $90^\circ$  counter clock wise in the lower right cell
- Place a copy of the curve rotated  $90^\circ$  clock wise in the lower left cell
- Place a copy of the curve on both upper cells
- Connect the 4 disjoint curves

This procedure can be repeated recursively up to the desired level, rotating the upper level cell back to its canonical shape.

If the basic unit of the Hilbert curve  $\square$  is replaced by an arc representing the connection of the entry and exit points, we can indicate the order by which all the points in a cell are going to be visited at a given level.

Considering the representation from Figure 7, the Hilbert indices can be calculated for a given point of interest in the following manner:

- a) Find the cell containing the point of interest, i.e. determining whether the point lies on the upper or lower half plane regarding each dimension. Assuming we are working on an order  $m$  curve, a point is represented by  $P = [p_0, p_1] \in \mathbf{B}^m * \mathbf{B}^m$ . Determining which half plane the point lies concerning the  $i^{th}$  coordinate is equivalent to determining the truth value of  $p < 2^{m-1}$ , which is equal to the  $(m-1)^{th}$  bit of  $p_i, bit(p_i, m-1)$
- b) Update key. Given the orientation at the current resolution (uniquely defined by the entry  $e$  and exit  $f$  of the curve through the lattice), we can determine the order under which each of the cells will be visited. Knowing that all points inside a cell are visited before moving on to the next cell, the index of the focused cell will tell whether the point of interest is visited in the first quarter of the curve or the second, and so on. In other words, we may determine two bits of the Hilbert index  $h$
- c) Transform as necessary. Knowing the index  $i$  of the cell under which the point of interest is located; we may determine the entry and exit points of the Hilbert curve through this cell. The cell is then transformed with a rotation, (expressed as an exclusive  $or$ ), and reflected (expressed as a bitwise rotation operation) back into its canonical orientation (entry in lower left, exit in lower right)
- d) Continue until enough precision was attained. Zooming in at the cell containing our point of interest, we can now inspect an order  $m-1$  Hilbert curve through a sub-cell of our original space. We repeat this procedure for each of the remaining  $m-1$  levels of precision, at each time calculating further 2 bits of the Hilbert index. At the end of the process, we have a  $2^m$  bit Hilbert index, isolating a single point on the curve of length  $2^{2^m}$  through the  $\mathbf{B}^m * \mathbf{B}^m$  lattice.

This algorithm can also be extended to further dimensions [6].



**Figure 7 - First four iterations of the 2D Hilbert curve in arc view**

# 4 METODOLOGY

---

## 4.1 iRT Overview

The iRT is part of a broader project IGIDE. The main goal of IGIDE is to develop a physically based global illumination renderer that is capable of generating accurate images at interactive rates within dynamic time-varying virtual models. Users should be able to navigate and interact within the virtual environment while visualizing perceptually accurate images that can be used in a predictive manner.

As a starting version in March 2009, iRT is single threaded application that traces single rays using work tasks in the form of rays or packets of rays, written onto a queue that feeds the rendering process to output an image. iRT is tracing single rays (scalar code) or packets of four rays (vectorized code based on SIMD extensions of the x86\_64 architecture), using BVH as the ADS to speed up the rendering time by reducing the number of ray-triangle intersections. The rays processing pipeline is depicted in Figure 8 and further described in the paragraphs bellow.

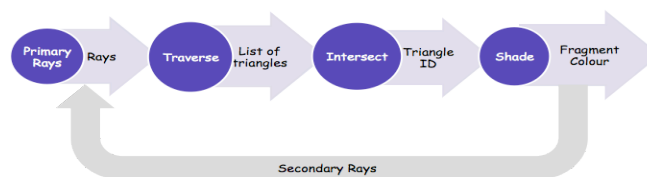


**Figure 8 - iRT Pipeline**

A module called “Camera” represents the image plane and generates the primary rays and adds them to a work queue. The ADS is then traversed to find the list of triangles belonging to the voxels touched by the ray. The selected triangles are then intersected with the rays to determine whether the rays actually intersect them or not and, in case they do, which are the closest to the rays’ origin.

The chosen triangles are then shaded according to its material and the light sources properties. In order to determine which light sources contribute to the final colour of the triangle, new rays are generated and added to the queue. Traversal, intersection and shading happen in the “Kernel” module.

The result of this processing is delivered to the “Film” component, responsible for providing the output to a screen window, a picture file or other medium. The architecture of the iRT is represented in Figure 9.

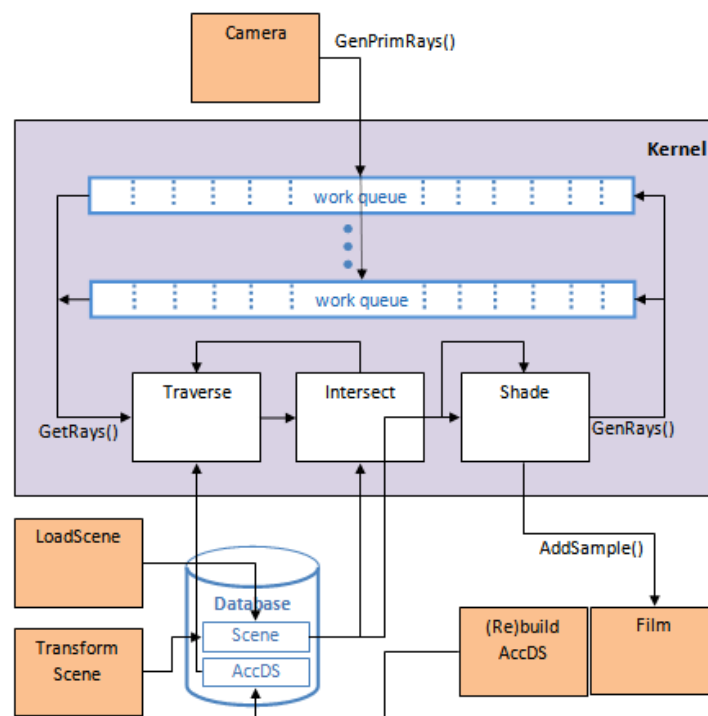


Figure 9 - Architecture of iRT

## 4.2 Workload decomposition

Parallel processing offers the potential of reducing computation time by employing more than one processor to solve the same problem. Because in ray tracing the computation of one pixel is completely independent of any other pixel, this algorithm tends to be greatly parallelizable and fit in a category known as embarrassingly parallel algorithms. A number of issues, which are not present in sequential programming, play an important role. Apart from correctness and robustness, efficiency and performance are of great importance. Choices must be made on the assignments and data decomposition and distribution.

In the context of ray tracing, decomposing the problem in independent tasks is the most common approach. This exploits the inherently parallel nature of the algorithm, by subdividing the image plane in smaller regions. With this approach, sequential algorithms can be easily parallelized and improvements on the sequential algorithm can be directly applied on the parallel approach. It also requires minimum communication between the processes, which allows a centralized approach and offers high scalability. On the downside, this approach has inherent issues with load balancing, as workload cannot be computed beforehand, scene must be replicated in every processor and poses challenges for techniques that require data from other regions, such as anti-aliasing.

Another approach, especially suited for big scenes, which do not fit in a single processors memory, is the decomposition of the objects in the scene. With this approach scene sizes can scale with the amount of processors, however, this requires complex designs and load balancing becomes a difficult challenge to overcome.

Control-oriented approaches are less common but also present in ray tracing, mostly in combination with one of the above. In this type of approaches, different processors are responsible for different tasks, such as collision detection and shading. An example of this approach being used together with image plane decomposition is given by Plachetka in [28], also described in section 3.8, to solve the antialiasing problematic with image space decomposition.

In the case of the ray tracer used within the context of this thesis, it was decided to use the image decomposition approach, since the ray tracer is used with small and medium static datasets, thus the scene can be easily replicated and there will be no repeated computation as the scenes are static.

### **4.3 Measuring efficiency of parallelization**

Let  $T_1$  be the execution time on 1 processor and  $T_n$  the execution time on  $n$  processors.

Speedup is given by  $S = \frac{T_1}{T_n}$ , expressing how much the overall performance increased with the

increase of processing power, whereas efficiency ( $E$ ) is given by  $E = \frac{S}{n} = \frac{T_1}{nT_n}$ , measuring

the speedup gained with the increase of the computational power. This definition gives

efficiency  $E = 100\%$  if increasing the number of processors  $p$  by a factor of  $n$  also increases the speed by the same factor. That is  $t_{np} = nt_p$ . When the efficiency is 100%, there is a linear relationship between  $n$  and  $t_{np}$ , meaning that the efficiency is independent from the number of processor and the speedup varies linearly with the number of processes.

If the efficiency can be held to near 100% then intuitively we feel we are getting a good return for the extra cost of the extra processors. If the efficiency declines from 100%, we feel that we are paying for more processors but we are not getting a proportional increase of speed.

## 4.4 Static Distribution

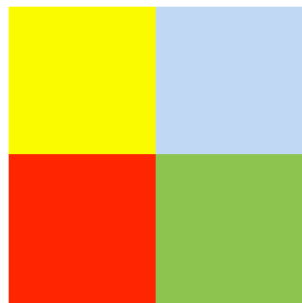


Figure 10 - Static Distribution

Node 1 Node 2 Node 3 Node 4

One of the simplest parallel implementation of a ray tracing is to simply replicate the entire scene in each processor and subdivide the workload into a number of disjoint tasks. Each processor then renders a number of rays using the unaltered sequential version of the ray tracing algorithm, until the whole frame is completed. Tasks are assigned based on the slave id, and thus do not require any communication to know which part it should work with. Each slave will always render the same sub region. The main advantage of this approach is the low communication cost, besides barely having to rewrite any code to go from a sequential to a parallel implementation. Communication is minimal as only the results of the completed tasks need to be transferred to a chosen processor that is responsible by sorting them in the correct order and deploying the final image to a film each frame. This is called static distribution.

The main issue regarding this approach is the load balance. In [29] is discussed two broad classifications of load balancing in the context of ray tracing for graphical rendering: data oriented parallelization and control-oriented parallelization. In the previous chapter, the choice of a data-oriented approach was explained. In this kind of approach tracing a single ray does

not seem to present great difficulties, but when it is done massively, it becomes an issue given that each ray may generate unpredictable large tasks, by adding several new rays to the work queue, while other rays leave the scene almost immediately after a single test. This generates considerable differences in the workload of independent processors. This is mainly due to diverse complexities of different sub regions of the image.

## 4.5 Static-Cyclic Distribution

When multiple computers operate in parallel to solve a single problem, some processors will eventually be more heavily loaded than the others. As a result, some processors may have no work left to do while others are still hardly working on the assigned task. Several methods of load balancing to alleviate this problem have already been studied. Although it is usually not possible to predict which subsets of rays will take the longest to trace, which makes it difficult to avoid a load imbalance problem. A static approach to alleviate load imbalances can be achieved by assigning multiple small regions for different areas of the image plane to each processor, instead of a single sub region. This way, if a given sub region is more complex its complexity will eventually be evenly distributed among all processors. The same is valid for simpler sub regions.

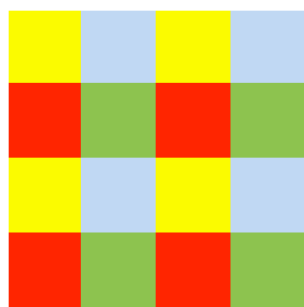


**Figure 11 - Static-Cyclic Distribution**

Consider the Figure 12, where the dark region represents a high load section. On the left we see the standard case of static distribution of work. Only Nodes 1 and 2 process the heavy load. On the right figure, we can see that by dividing the tasks in smaller chunks and assigning them cyclically, distributes the critical region among all processes. This approach, called Static-Cyclic, assigns tasks in a Round Robin fashion, a naïve approach to share critical regions among all processors.





**Figure 12 - Load Distribution with a Static-Cyclic approach**

## 4.6 Dynamic load balance

Another option to improve the load balance is to actively do so, adding software to even out the workload. This software entails having processors communicate with each other, sharing information about their current load and dynamically assigning the workload. Tasks can be distributed at runtime by a master processor. Whenever a processor finishes a sub region of the image, it asks the master processor for a new task. The master has a global vision of which sub regions have not been processed yet and assigns them on demand. This approach, known as demand-driven, benefits from a centralized awareness of the workload distribution, thus distributing it more efficiently. In this thesis, a slave is a processor responsible for rendering the image sub regions it has been assigned, either statically or dynamically. Slaves will generate rays and calculate their contributions to the image region. The master processor distributes tasks among the available slaves and gathers the results generated by them. Then it combines the results in a complete frame and outputs it. The master and all slaves are considered to have similar resources and properties. Although they can coexist in the same workstation, each will have exclusive access to one processing unit and memory is not shared. Although message-passing interfaces can implement optimizations that may use shared memory for communication between nodes in the same machine, these optimizations have not been used and thus each node is to be considered independent and communication is assumed to be the same between all processes.

In Figure 13 different loads have been assigned to each sub region, where the number displayed correspond to the time units it takes a slave to complete the task. We can see that node 1 had only 3 tasks while node 2 had 5, but the computational effort was the same for both of them. Speedups close to linear are expected with this approach as the overhead

introduced is minimal. Communication is ought to be minimal, thus it is expected that a large number of processors can be added before a bottleneck occurs.

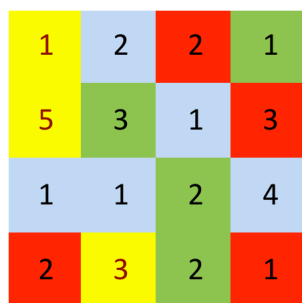


**Figure 13 - Dynamic Load Balancing**

Two main types of communication are needed in this approach: task distribution and results gathering. While the master node has tasks to be completed, it sends new tasks to the slaves that are idle. The second happens when the slave finished computing the results and sends its contribution back to the master. When the rendering of a frame starts, the master knows that every slave is free, and once a task has been sent, the master considers that the slave is busy. When a slave returns its results, the master knows that it is free again and can send more tasks. The master does the generation of the final frame gradually, every time it receives new results.

Three major issues were identified with this approach:

- At the beginning of each frame, slaves are idle until a new task is received. To overcome this, each slave will autonomously pick a given sub region, based on its id. Once the first task is complete, the results are sent to the master, that replies with the next task.
- A slave is idle between finishing a task and receiving a new one. To mitigate this idle time, each slave can be assigned more multiple tasks. If the master is expected to be highly loaded, more tasks can be assigned to each slave. This reduces the chances of the slaves being idle, but increases the likelihood of load imbalances. If the master is considered to be lightly loaded, just one task needs to be assigned to mitigate this problem. The ray tracer implemented in this thesis has just one task buffer.
- When distributing the last tasks of a frame, there is no room for load balancing, as no more tasks can be assigned to idle processors. Although this cannot be avoided, it can be mitigated by gradually refining the tasks size.

## 4.7 Tasks refinement

If a heavy task is assigned at the end of a frame to a given processor, the remaining processors will be idle waiting because there are no more tasks to distribute. One way to reduce the complexity of a task is to reduce the size of the region that must be rendered. This offers opportunity for other slaves to help with the critical region, while avoiding that a critical region has to be processed by a single slave at the end of the frame, when other slaves are idle. In our approach of tasks refinement, the tasks size decreases as depicted below.



Figure 14 - Task Refinement

## 4.8 Non-blocking communication

While the slaves are sending the results back to the master, they are idle until the message transmission is complete. The same is valid for the master, which cannot perform other tasks while it is receiving the results from the slaves. Message passing interfaces offer the possibility to have non-blocking communications, which means that processing can proceed while communications happen in the background. With careful redesign of the algorithm in order to avoid data concurrency, non-blocking communication was implemented. With the communication being done independently from the rendering (using non-blocking communication and overlapping communication with computation) then the communication costs become cheaper to a point of negligible to the overall processing impact.

## 4.9 Comparing Scan Line and Hilbert line traversal

Given the fact that primary rays share similar origins and the same direction, it is highly likely that consecutive rays will intersect the same triangle. In order to measure and visualize this fact, Figures 16 to 23 were generated, showing blue when two consecutive primary rays hit the

same triangle and black otherwise. This test was run both with a scan line and with a Hilbert curve traversal of the image plane.

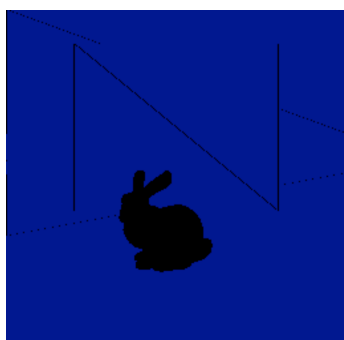


Figure 15 - Bunny - Scan Line

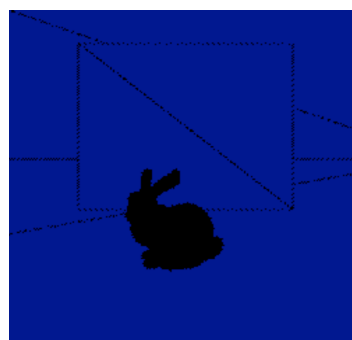


Figure 16 - Bunny - Hilbert Curve

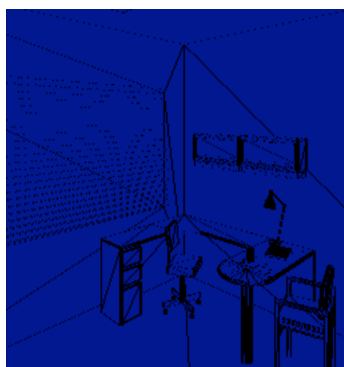


Figure 17 - Office - Scan Line

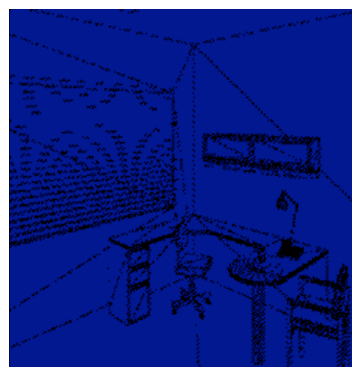


Figure 18 - Office - Hilbert Curve

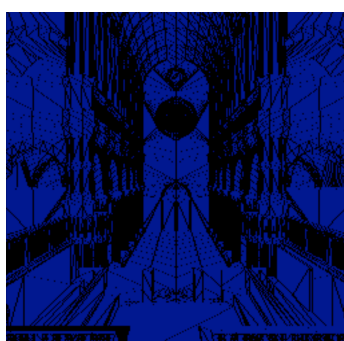


Figure 19 - Sibenik - Scan Line

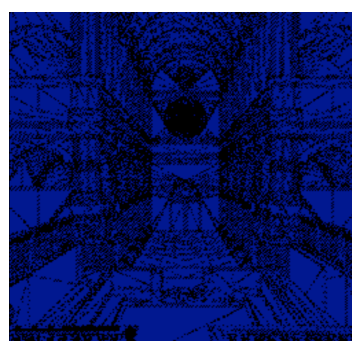


Figure 20 - Sibenik - Hilbert Curve

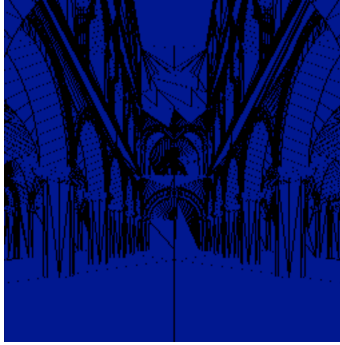


Figure 21 - Sponza - Scan Line

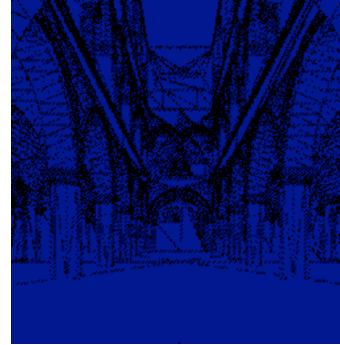


Figure 22 - Sponza - Hilbert Curve

The first thing that can be observed in the pictures is that there is a huge amount of coherence to be exploited. Most part of the pictures is blue, indicating us that repeated work exists, which can possibly be avoided. The following table shows the absolute count of blue dots for the studied scenes with the two proposed approaches. The results shown are for a resolution of 256 x 256 pixels, thus the total pixel count is 65 536.

**Table 1 - Coherence in Primary Rays**

Results	Bunny	Conference	Sibenik	Office	Sponza
Scan line	61662	53836	38427	59392	44016
Hilbert Line	61590	54168	40817	58335	45645
Coherence <sup>a</sup>	94%	83%	62%	89%	70%
Gain <sup>a</sup>	0.0%	0.1%	0.6%	-0.2%	0.4%

This confirms that there is actually great coherence in the traversal order of the screen plane, but shows us little advantage of the Hilbert line over the scan line, being sometimes even worst. Although this showed no promises of better exploitation of coherence with Hilbert lines, optimizations were designed and implemented given that so much coherence is available in the primary rays. The most costly part in ray tracing is traversing the ADS<sup>10</sup>, where several tests

$$Coherence(\%) = \frac{Max(Scanline, Hilbert) * 100}{Tpixels}$$

$$Gain(\%) = \frac{Hilbert * 100}{Scanline} - 100$$

<sup>10</sup> A BVH is used in this example but the same technique can be applied to other ADS such as KD-trees

have to be made to find all the triangles that a ray intersects. It is then necessary to determine which of the triangles is the closest to the ray origin (all the others will be occluded by the first one and thus will not contribute to the current ray). In the ray tracer used in this thesis, finding the closest triangle to the ray source was done in two steps: first determining the list of triangles intersected by the ray and then identifying which one is closer. Both steps were combined in a single one, since once the ray hits a triangle, the maximum distance a triangle is worth being tested is known, given that any other triangle that is farther will certainly be occluded. Following this principle, any AABB of which the nearest plane, regarding the ray's origin, is further than an already intersected triangle can be safely ignored, since any triangle the ray might intersect will certainly be farther. This optimization, referred as PET (Primary Early Termination), can greatly reduce the overall number of traversal steps. As stated before in section 3.4, two consecutive rays share similar origins and the same directions; therefore it is highly likely that they intersect the same triangle. Thus a new ray could be intersected with the closest triangle of the previous ray. If the new ray also intersects the same triangle we can start the ADS traversal with a PET condition, thus reducing even more the necessary traversal steps, with the small cost of storing the closest triangle and intersecting it with the new ray at the beginning of the ADS traversal of the next ray.

“The power of classical ray tracing comes from the fact that the illumination signal is computed anew for each shading point. The direct light sources are stratified and sampled, and the indirect environment is sampled (or approximated from prior evaluations). This means that the method can capture sharp shadows; when a point no longer sees a source, it falls automatically into shadow, and if the source is sufficiently small, the shadow will be sharp. Specular reflections and refractions are also easily captured, since the proper illumination directions are evaluated when needed. All of these components of the illumination signal may be refined adaptively to any level of precision and confidence.” [30].

With this in mind, a similar approach to PET can be applied to hard shadow rays, with a significant difference: a shadow ray is generated for each light source, thus the triangle is kept for each light source. For each shadow ray targeting a given light source, it is first tested against the stored triangle (no test is made if the last shadow ray hit the light source). If successful, the ADS is not traversed, as an occlusion has already been found. This optimization is referred as OCC (Occlusion Culling). Given that the order primary rays are

processed determines the order secondary rays are generated, the traversal order of the image plane directly influences the efficiency of this approach.

One last optimization used is called SET (Shadow Early Termination). In the case of shadow rays, it is sufficient to know if the origin of the ray is occluded or not, i.e. if the shadow ray hits any triangle. If so, the traversal of the ADS can be stopped as soon as a collision is found. This approach has two advantages: first, it prevents unnecessary traversal steps of the ADS. Second, the triangle with which the ray collided, and that is going to be used by the OCC, is not necessarily the closest to the ray origin. The triangle size and orientation can vary, but assuming that they have the same size and orientation, the further they are from the shadow rays origin, and thus closer to the light source, the bigger the chance that it will occlude more rays coming from nearby sources. This directly benefits the efficiency of the OCC algorithm.

# 5 RESULTS

---

## 5.1 Experimental Setup

The following tests were performed in the Search Cluster at University of Minho<sup>11</sup>. They were performed in a cluster with 8 Quad-Core Xeon E5130 with 4 GB of Ram, connected with a 10Gbps Myrinet network. All the results presented are the median value of 10 executions.

## 5.2 Load Balancing

In tables 2 to 5 we can see the results of applying the different load balancing approaches to the different scenes.

---

<sup>11</sup> More information in <http://search.di.uminho.pt/>



**Table 2 - Load Balancing – Bunnies**

<b>Results (FPS/Efficiency<sup>12</sup>)</b>	<b>1 Slave</b>	<b>2 Slaves</b>	<b>4 Slaves</b>	<b>16 Slaves</b>	<b>32 Slaves</b>
1: Static	1,0444 N/A	1,6438 78,6946%	2,879 68,9153%	11,086 66,3429%	20,1752 60,3683%
2: Static-Cyclic	1,0406 N/A	1,9204 92,275%	3,8353 92,144%	14,4389 86,7261%	27,9661 83,9882%
3: Dynamic	1,0482 N/A	2,0324 96,9497%	4,0213 95,9113%	15,4969 92,4054%	27,78 82,8236%
4: 3 + Overlap of Comp. w/ Comm.	1,0444 N/A	2,0848 99,8064%	4,1741 99,9154%	16,9526 101,4496%	32,6008 97,5468%
5: 4 + Non-Blocking Comm.	1,0494 N/A	2,0861 99,3921%	4,2178 100,4795%	17,0632 101,625%	32,9571 98,1431%
6: 5 + Task refinement	1,0502 N/A	2,0851 99,2751%	4,1857 99,644%	17,1271 101,9335%	31,6754 94,2595%

<sup>12</sup> Efficiency described in section 4.3

**Table 3 - Load Balancing – Office**

<b>Results (FPS/Efficiency)</b>	<b>1 Slave</b>	<b>2 Slaves</b>	<b>4 Slaves</b>	<b>16 Slaves</b>	<b>32 Slaves</b>
1: Static	0,4181 N/A	0,7862 94,0244%	1,3608 81,3762%	4,5649 68,2489%	8,5921 64,2303%
2: Static-Cyclic	0,4186 N/A	0,8207 98,0349%	1,6196 96,7365%	6,3354 94,6049%	12,5239 93,509%
3: Dynamic	0,4185 N/A	0,8253 98,6151%	1,6396 97,966%	6,5802 98,292%	12,7267 95,0538%
4: 3 + Overlap of Comp. w/ Comm.	0,4169 N/A	0,8216 98,5422%	1,6531 99,1408%	6,768 101,4786%	13,3812 100,318%
5: 4 + Non-Blocking Comm.	0,4197 N/A	0,8264 98,4681%	1,6523 98,4376%	6,7887 101,1138%	13,4203 99,9451%
6: 5 + Task refinement	0,4188 N/A	0,8398 100,2703%	1,6859 100,6447%	6,8537 102,2915%	13,6187 101,6296%

**Table 4 - Load Balancing - Sibenik**

<b>Results (FPS/Efficiency)</b>	<b>1 Slave</b>	<b>2 Slaves</b>	<b>4 Slaves</b>	<b>16 Slaves</b>	<b>32 Slaves</b>
1: Static	0,4926 N/A	0,9685 98,3%	1,7729 89,973%	6,5675 83,3264%	12,7821 81,0886%
2: Static-Cyclic	0,4930 N/A	0,9757 98,9605%	1,9123 96,9802%	7,5436 95,641%	14,7627 93,5848%
3: Dynamic	0,4913 N/A	0,9797 99,7168%	1,9166 97,5412%	7,6176 96,9217%	14,8029 94,1716%
4: 3 + Overlap of Comp. w/ Comm.	0,4937 N/A	0,9854 99,81%	1,9835 100,4515%	7,9782 101,0146%	15,8631 100,425%
5: 4 + Non-Blocking Comm.	0,4949 N/A	0,9865 99,6639%	1,9845 100,249%	8,0124 101,1875%	15,91 100,4637%
6: 5 + Task refinement	0,4943 N/A	0,9884 99,9873%	1,9797 100,1373%	7,9775 100,8814%	15,8348 100,1222%

**Table 5 - Load Balancing – Sponza**



<b>Results (FPS/Efficiency)</b>	<b>1 Slave</b>	<b>2 Slaves</b>	<b>4 Slaves</b>	<b>16 Slaves</b>	<b>32 Slaves</b>
1: Static	0,3960 N/A	0,7648 96,5671%	1,3287 83,8822%	4,9544 78,1978%	9,4552 74,6185%
2: Static-Cyclic	0,3981 N/A	0,7829 98,3203%	1,5664 98,3641%	6,1088 95,9054%	11,914 93,5236%
3: Dynamic	0,3978 N/A	0,7716 96,9986%	1,5216 95,6481%	6,0421 94,953%	11,562 90,8499%
4: 3 + Overlap of Comp. w/ Comm.	0,3974 N/A	0,7838 98,6286%	1,5936 100,261%	6,4522 101,4898%	12,733 100,1418%
5: 4 + Non-Blocking Comm.	0,3977 N/A	0,7905 99,389%	1,5961 100,337%	6,483 101,8884%	12,7882 100,492%
6: 5 + Task refinement	0,3973 N/A	0,7949 100,0485%	1,592 100,1865%	6,503 102,312%	12,8608 101,1701%

It is clear that the Static approach holds the lowest performance, mainly due to load imbalances. In can be observed that by just applying a cyclic distribution of tasks, an improvement of 20% to 30% of the efficiency of the parallel algorithm. The results where the efficiency raises above 100% can be explained with the overhead existing in running the ray tracer with just one slave, where the communication overhead already exists. We can also observe that in the case of the Bunny, the tasks-refinement held worst results than without it. This is understandable given that the last tasks, the bottom right corner, are covered by a single triangle. This gives no advantage to the approach and increases the overhead of the algorithm, as a single triangle has to be processed by multiple processors.

### 5.3 Spatial Coherence

To understand how much coherence exists, a colour map was implemented, colouring the image according to the number of light sources occluded by the same triangle in consecutive rays. The following images show on the left side the results of the scan line order and on the right side the results of the Hilbert line order for five scenes, in order of appearance: Bunny, Conference, Sibenik, Office, Sponza.

The colours represent:

- |  |  |
|--|--|
|  1 Light Source Occluded  |  2 Light Sources Occluded         |
|  3 Light Sources Occluded |  4 Light Sources Occluded         |
|  5 Light Sources Occluded |  6 Light Sources Occluded         |
|  7 Light Sources Occluded |  8 or more Light Sources Occluded |

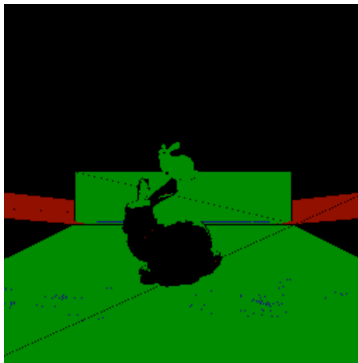


Figure 23 - Bunny - Scan Line

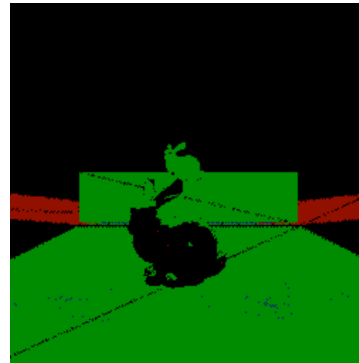


Figure 24 - Bunny - Hilbert Curve

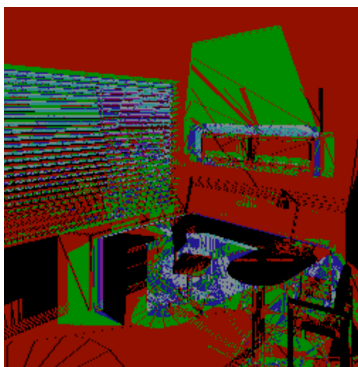


Figure 25 - Office - Scan Line

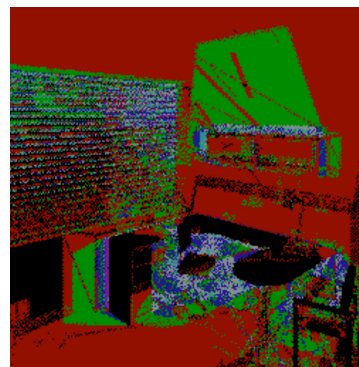


Figure 26 - Office - Hilbert Curve

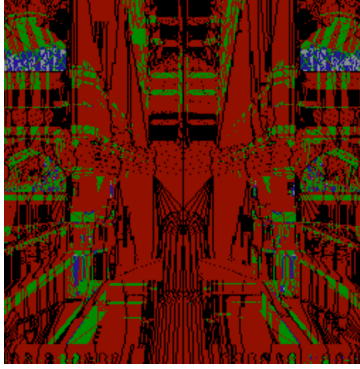


Figure 27 - Sibenik - Scan Line

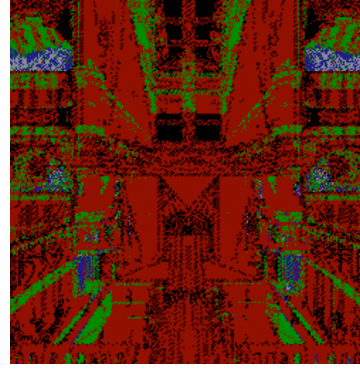


Figure 28 - Sibenik - Hilbert Curve

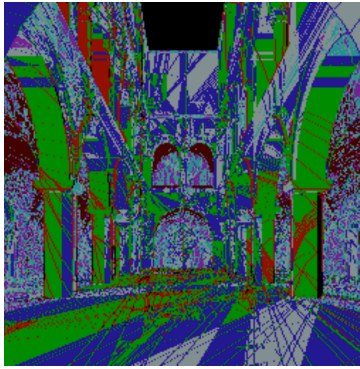


Figure 29 - Sponza - Scan Line

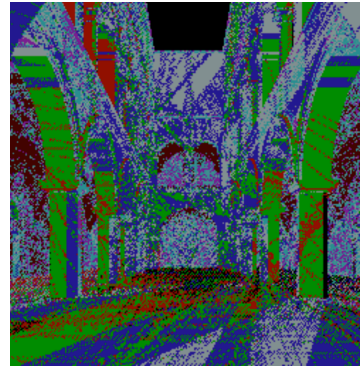


Figure 30 - Sponza - Hilbert Curve

In the tables bellow, the same results are represented numerically.

**Table 6 - Spatial Coherence with Scan Line Traversal**

<b>Results</b>	<b>Bunny</b>	<b>Office</b>	<b>Sibenik</b>	<b>Sponza</b>
Primary Rays	61662	59392	38427	44016
1 Light Source	1758	31639	39161	5093
2 Light Sources	26967	12850	7609	18237
3 Light Sources	152	3608	1200	17728
4 Light Sources	0	2466	391	10708
5 Light Sources	0	1521	0	3968
6 Light Sources	0	569	0	2802
7 Light Sources	0	877	0	1787
8+ Light Sources	0	821	0	6920
Total <sup>13</sup>	56148	98736	59543	212424

<sup>13</sup> The total is the sum of successes multiplied by the number of lights. E.g. In the case of the scan line for the bunny scene, Total = 1x1758 + 2x26967 + 3x152 = 56148.

**Table 7 - Spatial Coherence with Hilbert Curve Traversal**

Results	Bunny	Office	Sibenik	Sponza
Primary Rays	61590	58335	40817	45645
1 Light Source	1725	32051	41049	5216
2 Light Sources	27061	12673	8552	16841
3 Light Sources	91	3607	1457	15888
4 Light Sources	0	1997	614	11134
5 Light Sources	0	1072	0	4827
6 Light Sources	0	429	0	3038
7 Light Sources	0	472	0	2077
8+ Light Sources	0	416	0	8385
Total	56120	89176	64980	220388

Table 8 shows the gain of the Hilbert Curve traversal in comparison to the Scan Line traversal. The gain is calculated with the following formula:

$$Gain(\%) = \frac{Hilbert * 100}{Scanline} - 100$$

**Table 8 – Gain of Traversing the Image Plane with the Hilbert Curve against Scan Line**

Results	Bunny	Office	Sibenik	Sponza
Primary Rays	-0,1168	-1,7798	6,2196	3,701

These results show that although the approach changes the performance of the algorithm, it does not conclude under which conditions each algorithm is better.



Below are the results of applying the above cited techniques for exploiting coherence, i.e., SET, OCC and PET, for different scenes with different numbers of light sources.

**Table 9 - Exploiting Coherence with Scan Line Traversal**

<b>Results (FPS/Gain)</b>	<b>Bunny 3 LS</b>	<b>Office 8 LS</b>	<b>Sibenik 4 LS</b>	<b>Sponza 8 LS</b>
Base	1,0444	0,4181	0,4926	0,3960
SET	1,2148 16,3142%	0,5158 23,3670%	0,5751 16,7463%	0,6226 57,2009%
OCC	1,2921 23,7161%	0,5572 33,2636%	0,6355 29,006%	0,6815 72,0758%
PET	1,0546 0,9686%	0,426 1,8851%	0,5441 10,4534%	0,4113 3,8540%
OCC-PET	1,3088 25,3155%	0,5741 37,2955%	0,7234 46,8477%	0,7294 84,1785%
SET-OCC-PET	1,3071 25,1467%	0,5745 37,4002%	0,7246 47,0925%	0,7307 84,5166%

**Table 10 - Exploiting Coherence with Scan Line Traversal**

<b>Results (FPS/Gain)</b>	<b>Bunny 3 LS</b>	<b>Office 8 LS</b>	<b>Sibenik 4 LS</b>	<b>Sponza 8 LS</b>
Base	1,0413	0,4203	0,5091	0,3964
SET	1,2216 17,3103%	0,518 23,2305%	0,5943 16,7331%	0,6241 57,4298%
OCC	1,2891 23,7922%	0,5507 31,0216%	0,6763 32,8405%	0,7017 77,0081%
PET	1,0577 1,5705%	0,4285 1,9446%	0,5632 10,6246%	0,4132 4,2169%
OCC-PET	1,318 26,5638%	0,569 35,3643%	0,7881 54,7834%	0,7665 93,3401%
SET-OCC-PET	1,3137 26,1501%	0,5689 35,3384%	0,7883 54,8289%	0,7649 92,9385%

The results show that the spatial coherence present in the scene can be exploited. In fact results have shown performance improvements of over 90% when many light sources are present in the scene. The most successful approach exploiting coherence was the occlusion culling. When combined with the PET approach, the improvements correspond to the cumulative improvement of each algorithm, showing that they complement each other. As for the SET approach, it seems to lose significance when the occlusion culling is also present. This is expected as they both exploit the same feature, which is the fact that consecutive shadow rays to a given light source are often occluded by the same triangle.

As for the difference between the scan line and the Hilbert curve traversals, the tests show that there is no significant advantage of one over the other. This was already expected given the results shown in Table 6.

The tested approaches might have not been the best, given that they only benefit two consecutive rays, which is still a one-dimensional approach. Optimizations that would target a given region, where the two dimensions influenced the efficiency of the approach, would possibly benefit the Hilbert Curves.

# 6 CONCLUSIONS

---

## 6.1 Achieved goals

This study has shown that iRT could be successfully parallelized, achieving linear speed-ups, as expected given the embarrassingly parallel nature of the algorithm. To achieve such speed-ups, the resort to multiple techniques was necessary. Those include:

- Dynamic load balancing
- Efficient work load decomposition
- Adaptable tasks granularity
- Non-blocking communication

To the success of this approach much contributed the high performance of the network, that kept the communication costs to a minimum and the efficiency of the Message Passing Interfaces, that allowed to scale the application between different processors but also cores within the same processor.

This studied also demonstrated the significant amount of coherence existent in the image plane and how the image plane traversal order can change the efficiency of optimizations that thrive on such spatial coherence. Strategies such as PET, OCC and SET improve the efficiency of the algorithm, avoiding unnecessary computation, thus increasing the overall performance. The amount of spatial coherence identified leaves the door open for other optimizations that benefit from properties that are common to objects that appear near in the image plane.

## 6.2 Future work

Results have shown that the traversal algorithm has impact on the performance of the proposed coherence optimizations, although it was not clear under which circumstances each approach thrives. It is suggested as a future work that the strengths and weaknesses of each approach are identified and exploited.

Although the optimizations designed and implemented work on a bi-dimensional plane, the benefits are available only for two consecutive rays. Locality could be better exploited with algorithms that cover an area, for instance an anti-aliasing algorithm. Such approaches could potentially further benefit from the Hilbert curve traversal order.

# 7 BIBLIOGRAFY

---

- [1] A. Oliveira, L. P. Santos, and A. Proença, “Refinement criteria for high fidelity interactive walkthroughs,” presented at the GRAPHITE '06: Proceedings of the 4th international conference on Computer graphics and interactive techniques in Australasia and Southeast Asia, 2006.
- [2] T. Whitted, “An improved illumination model for shaded display,” *Seminal graphics*, Jul. 1998.
- [3] M. J. Muuss, “Towards Real-Time Ray-Tracing of Combinatorial Solid Geometric Models,” *Proceedings of BRL-CAD Symposium*, pp. 1–15, Feb. 2008.
- [4] Keates, “Interactive Ray Tracing on a Virtual Shared-Memory Parallel,” pp. 1–14, Nov. 2007.
- [5] G. Peano, “Sur une courbe, qui remplit toute une aire plane,” *Mathematische Annalen*, vol. 36, no. 1, pp. 157–160, Mar. 1890.
- [6] Hamilton, “Compact Hilbert indices: Space-filling curves for domains with unequal side lengths,” *Inf Process Lett*, vol. 105, no. 5, pp. 9–9, Feb. 2008.
- [7] J. Bigler, A. Stephens, and S. G. Parker, “Design for Parallel Interactive Ray Tracing Systems,” *Interactive Ray Tracing 2006, IEEE Symposium on*, pp. 187–196, 2006.
- [8] I. Wald, P. Slusallek, C. Benthin, and M. Wagner, “Interactive Rendering with Coherent Ray Tracing,” *Computer Graphics Forum (Proceedings of EUROGRAPHICS)*, vol. 20, no. 3, pp. 153–164, 2001.
- [9] A. Reshetov, “Multi-Level Ray Tracing Algorithm,” pp. 1–10, Sep. 2005.
- [10] O. Karlik, “Utilization of generic programming in Ray Tracing,” 2009.
- [11] I. Wald, S. Boulos, and P. Shirley, “Ray tracing deformable scenes using dynamic bounding volume hierarchies,” *ACM Transactions on Graphics (TOG)*, vol. 26, no. 1, p. 6, 2007.
- [12] I. Wald, W. R. Mark, J. Günther, S. Boulos, T. Ize, W. Hunt, S. G. Parker, and P. Shirley, “State of the Art in Ray Tracing Animated Scenes,” *Eurographics 2007 State of the Art Reports*, vol. 28, no. 6, pp. 1691–1722, 2009.
- [13] M. Nunes, L.P. Santos, “Workload distribution for ray tracing in multi-core systems,” 2009.
- [14] I. Wald, P. Slusallek, C. Benthin, and M. Wagner, “Interactive distributed ray tracing of highly complex models,” pp. 277–288, 2001.
- [15] K. Dmitriev, V. Havran, and H.-P. Seidel, *Faster Ray Tracing with SIMD Shaft Culling*. 2004.

- [16] A. Reshetov, "Faster Ray Packets - Triangle Intersection through Vertex Culling," *CORD Conference Proceedings*, pp. 105–112, Sep. 2007.
- [17] S. Boulos, I. Wald, and P. Shirley, "Geometric and arithmetic culling methods for entire ray packets," *University of Utah*, 2006.
- [18] I. Wald, C. P. Gribble, S. Boulos, and A. Kensler, "SIMD Ray Stream Tracing-SIMD Ray Traversal with Generalized Ray Packets and On-the-fly Re-Ordering," *SCI Institute, University of Utah, Technical Report# UUSCI-2007-012 (Aug. 2007)*, pp. 1–8, 2007.
- [19] M. A. Z. Dippé and E. H. Wold, "Antialiasing through stochastic sampling," presented at the SIGGRAPH '85: Proceedings of the 12th annual conference on Computer graphics and interactive techniques, 1985.
- [20] D. P. Mitchell, "Generating antialiased images at low sampling densities," vol. 21, no. 4, pp. 65–72, 1987.
- [21] J. Painter and K. Sloan, "Antialiased ray tracing by adaptive progressive refinement," vol. 23, no. 3, 1989.
- [22] F. P. Preparata and M. I. Shamos, "Computational geometry: an introduction," *Computational geometry: an introduction*, Sep. 1985.
- [23] Y. Y. Eldar, M. M. Lindenbaum, M. M. Porat, and Y. Y. Y. Zeevi, "The farthest point strategy for progressive image sampling.," *IEEE Trans Image Process*, vol. 6, no. 9, pp. 1305–1315, Dec. 1996.
- [24] I. Notkin and C. Gotsman, "Parallel Progressive Ray-tracing," vol. 16, no. 1, pp. 43–55, 1997.
- [25] T. Plachetka, "Perfect load balancing for demand-driven parallel ray tracing," *Euro-Par 2002 Parallel Processing*, pp. 91–120, 2002.
- [26] "Space-filling curve," *Wikipedia.org*. [Online]. Available: [http://en.wikipedia.org/wiki/Space-filling\\_curve](http://en.wikipedia.org/wiki/Space-filling_curve). [Accessed: 20-Oct.-2012].
- [27] J. Arvo, "Graphics Gems II - James Arvo - Google Books," 1991.
- [28] T. Plachetka, "Tuning of algorithms for independent task placement in the context of demand-driven parallel ray tracing," presented at the EG PGV'04: Proceedings of the 5th Eurographics conference on Parallel Graphics and Visualization, 2004.
- [29] D. Badouel, K. Bouatouch, and T. Priol, "Distributing data and control for ray tracing in parallel," *Computer Graphics and Applications, IEEE*, vol. 14, no. 4, pp. 69–77, 1994.
- [30] A. S. Glassner, *Principles of Digital Image Synthesis*. 1995.